Detailed Analysis of Heat Flow Pattern in a Piston

T.Morel, R.Keribar

Ricardo-ITI, Inc.
645 Blackhawk Drive
Westmont, IL 60559
U.S.A.

S.T.Harman

Chrysler Motors, Highland Park, MI

ABSTRACT

Temperature and heat flow distribution were studied analytically in a piston of an S.I. engine. An advanced engine simulation code was used, which solves for engine performance, calculates thermal boundary conditions, and simultaneously obtains detailed temperature distributions by a finite element (FE) structure heat conduction solution built into the simulation. The FE solution is obtained simultaneously for piston, cylinder, head and valves, and thus all of their thermal interactions are accounted for and heat flow patterns are revealed. The engine was simulated at two engine speeds at wide open throttle (WOT) conditions, and the results were compared to experiments. The results showed the details of heat paths in the piston, produced by the deposition of heat flux from combustion gases and of frictional heat. This heat flows to the two primary heat sinks, i.e., cylinder block coolant and sump oil. The split of the heat fluxes from the sources to the sinks through the piston/cylinder assembly is discussed.

INTRODUCTION

With the trend toward higher specific output and lightweight component construction, the design of engine components requires careful attention. There is increasing use of finite element (FE) analysis (Li, 1982; Groeneweg et al., 1987; Li, 1988; Hosokawa et al., 1989), in which the component is discretized into many small volumes (elements) and governing equations are solved to obtain temperature and stress distributions. The component may be made of uniform material or may be a composite (Keribar et al., 1990), and it can be studied under steady-state or transient conditions (Keribar and Morel, 1987). The FE method is a mature tool and it can represent thermal and structural behavior under all of the above conditions.

The primary use of FE as applied to pistons is to obtain predictions for temperature distributions and for predictions of thermal and mechanical stresses. Another use of this analysis is to assess the general directions in which heat flows through the assembly. This is important in the evaluation and optimization of piston cooling strategies, e.g., cylinder cooling or oil piston cooling.

This paper describes the FE analysis of an automotive aluminum piston coupled with performance analysis. The piston was modeled within the context of the surrounding components, i.e., including the cylinder and the head. The piston temperature predictions were compared to available data. The main objective of this paper is to discuss the application of boundary conditions and also to analyze the predicted heat paths through the piston and at the piston/cylinder interface.

ENGINE PARAMETERS

The engine studied was the Chrysler 2.2ℓ 4-cylinder engine, characterized by the following parameters:

Bore (mm)	87.5
Stroke (mm)	92.0
Connecting rod length (mm)	151.0
Compression ratio	9.61
Displacement (ℓ/cyl)	0.553

The engine has two valves per cylinder, placed in a wedge-type depression in the head.

The two engine operating conditions considered for performance (and FE) analysis were the WOT at 4800 RPM and 3000 RPM. Engine operating parameters used for both conditions were based on engine dynamometer data. These were used to set up the input file for the simulation, which provided the needed boundary conditions for the FE calculations. All of the calculations (performance and thermal FE) were carried out using Ricardo-ITI's engine simulation code IRIS, which has been described by Morel et al., 1988A and is further discussed below.

The operating parameters of the engine for which the analysis was carried out are given in Table I. These two nominal operating points have been chosen because measured temperature data obtained at Musashi Institute of Technology (Furuhama, 1989) are available. These data are compared below with the predicted temperatures.

Table I. Operating Parameters of the Engine and Predicted Performance

RPM	3000	4800
Spark timing (°BTDC)	21.5	19.1
A/F ratio	11.8	13.8
BHP	78.9	108.4
Peak pressure (bar)	66.0	64.0

PISTON AND ITS FE REPRESENTATION

The piston of the 2.2ℓ engine is made of a cast aluminum alloy and contains a steel strut which surrounds the pin boss. The piston has a flat crown with a shallow depression for valve clearance, a cutout skirt, and three rings. Nominal diameter and height of the piston are 87.5 mm and 71.3 mm, respectively.

Finite Element Representation

A three-dimensional half model of the Chrysler piston was generated using linear, isoparametric solid finite elements (hexahedra, pentehedra and tetrahed- ra). The model consists of 2293 nodal points and 1842 elements and is shown in Figures 1 and 2. This level of resolution is considered medium to high and is appropriate for thermal analysis of the piston. Most features of the geometry (including the pin offset) have been represented except for some fillets and fine details or imperfections on cast (unmachined) surfaces. Also not modeled was the steel strut, i.e., the piston was assumed to be made entirely of aluminum. This should not have a significant

effect on the resulting temperatures, although it would impact piston distortions and stresses.

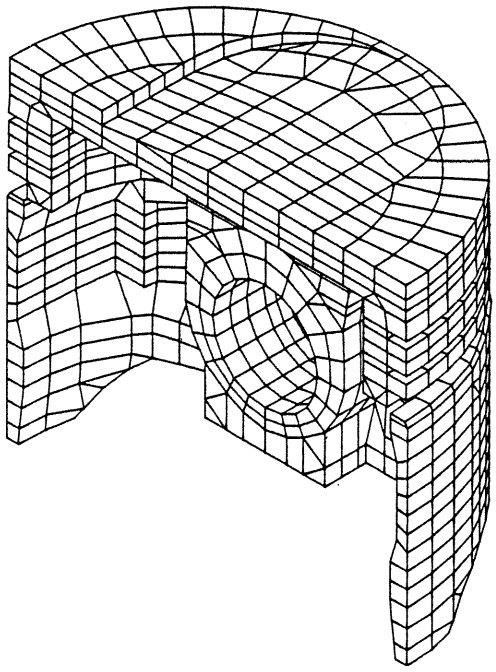

Figure 1. Half model of piston: orthographic view showing piston crown, pin boss and skirt.

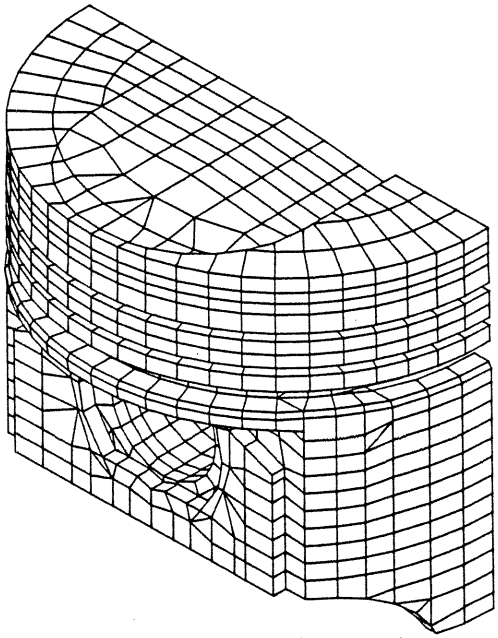

Figure 2. Half model of piston: orthographic view showing piston crown, ring lands/grooves and skirt.

For purposes of thermal analysis and correct application of thermal boundary conditions, the piston FE model was augmented by a scalar element representation of the rest of the engine structure (rings, block, head, valves, and ports). To account for the heat paths between the piston and cylinder, scalar thermal connectivities were applied between all nodes on the piston skirt/ring and cylinder nodes facing the combustion chamber. Thermal contact between piston and rings was also modeled by scalar connectivities connecting ring groove side nodes to ring nodes in the network. With the network representation of the structure merged to the piston FE model, the number of nodes increased to 2686. At the same time, 1756 scalar elements were added, increasing the total number of elements to 3598.

It should be noted that the block of this engine has siamesed cylinders, i.e., the coolant does not circulate all around the cylinder. This means that the cooling is not axisymmetric and as a result the thrust and antithrust surface areas are well cooled, while higher cylinder surface temperatures may be expected on the areas of the cylinder in siamese contact. However, in this work the cylinder was represented, for simplicity, by an axisymmetric shell cooled uniformly around the circumference.

ANALYTICAL METHODOLOGY

To carry out the simulations presented in this paper, an integrated performance/FE engine simulation methodology IRIS was used, described in Morel et al., 1988A. This simulation links, in a fully consistent way, a detailed thermodynamic model of in-cylinder processes with finite element structural analysis. The performance model calculates the requisite thermal boundary conditions and feeds them to the FE solver; in return the FE solution provides the surface temperatures needed for wall-to-gas heat transfer calculations. A summary of the key features of the IRIS methodology is given below.

Thermodynamic Analysis

Engine heat transfer is driven by the air flow and combustion phenomena. Because of that, the heat transfer methodology is implemented in the detailed thermodynamic simulation of the engine operation. This model provides time-resolved information about combustion chamber pressure, temperature and thermodynamic properties (separately for burned and unburned gases), flow velocities and mass flow through valves, intake angular momentum flux, details of the injection process, as well as the instantaneous piston location and chamber geometry. The structural heat transfer calculations, which are coupled to IRIS, feed back into the thermodynamic analysis through the heat transfer term in the energy equation. Therefore, they have an effect on the piston work, exhaust temperatures, as well as component temperatures.

Combustion Model

For spark ignited engines the simulation uses a variant of the turbulent flame propagation model (Morel et al., 1988B). This model calculates the rate of burn as a product of the instantaneous flame area, turbulent flame speed and unburned gas density. The instantaneous flame area is calculated by a geometrical model which can represent complex head or piston geometries. The flame speed utilizes predicted turbulent intensity and length scale calculated by a turbulence model.

Convective Heat Transfer Model

The convective heat transfer model is based on an in-cylinder flow model which computes swirl, squish and turbulence as a function of crank angle (Morel and Keribar, 1985 and Morel et al., 1988B). It provides key spatial dependence, in that it divides the cylinder into four flow regions (squish region above piston crown, piston cup volume, head depression volume, and region above the cup), and solves differential equations in each for swirl and turbulence. Its main features are: (1) the inherent dependence of the convective heat transfer on the actual flow velocities, and (2) the spatial resolution, which this allows, including the capability to treat re-entrant piston bowl shapes. A total of forty distinct in-cylinder surfaces are accounted for, with a separate heat transfer coefficient calculated for each. An additional convective heat transfer model calculates heat transfer between port gases and port surfaces. For diesel applications, a detailed radiative heat transfer model calculates the separate contribution of heat radiation.

Structural Heat Conduction

Steady-state or transient conduction through the engine structure is calculated in IRIS via the FE method which is suitable for representation of geometrical detail as well as differentiating materials through property specification. Any FE code (such as NASTRAN or ANSYS) can be used to generate a geometrical representation of part of the engine structure or component of interest. There are no limitations on the FE model;

large 3-D models with many thousands of nodes can be accommodated. An internal pre-processor generates a coarser, scalar FE model of the remainder of the engine structure. Such representations can be constructed by the pre-processor for any diesel or SI engine geometry using a library of component submodels. The scalar FE model can also be selected for representing the entire engine structure, as was done here. This approach results in CPU time economies, allowing both concept-stage and detailed multi-dimensional design-stage thermal analyses of components to be carried out simultaneously and coupled with performance analysis of the engine, both for steady state and for transient operation.

PISTON THERMAL LOAD

The thermal load on the piston provides the boundary conditions for thermal FE calculations. The gas side and frictional (heat generation) thermal loads are computed within IRIS and are automatically applied to the FE piston model gas side and friction surfaces. The piston crown convective boundary condition is applied in IRIS in the form of surface heat transfer coefficients and a convective temperature on eight piston zones. These zones distinguish between inner and outer crown surface and also define major thrust, "front", minor thrust and "back" quad- rants, as shown in Figure 3. These divisions can account for spatial variation of flow velocities (due to squish and swirl motions) in the calculation of convective heat transfer coefficients and also for effects of spark location on local convective temperatures. Predicted distribution of cycle-average effective convective heat transfer coefficients and temperatures for these surfaces are shown in Table II.

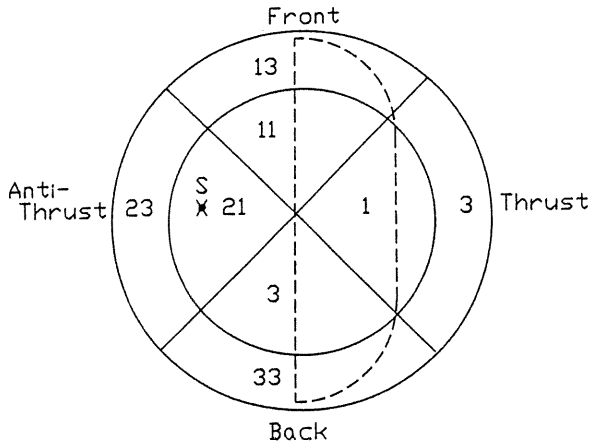

Figure 3. Piston surface breakup used in IRIS for the application of combustion chamber gas thermal boundary conditions. Spark location and piston valve clearance cutouts have been superimposed on the figure.

Table II. Piston-Top Thermal Boundary Conditions

Surface ID	4800 RPM, WOT		3000 RPM, WOT	
	T_{gas}(K)	h_{gas}(W/m^{2}K)	T_{gas}(K)	h_{gas}(W/m^{2}K)
1	1643	639	1508	443
11	1696	630	1559	439
21	1738	623	1599	433
31	1696	630	1559	439
3	1386	666	1271	463
13	1567	635	1436	441
23	1664	618	1526	429
33	1567	635	1436	441

Note the higher convective temperatures for surfaces 21 and 23 which are on the side closest to the spark plug, versus surfaces 1 and 3 on the opposite side. The variation of instantaneous convective heat transfer coefficient and temperature with crank angle for the four outside surfaces at the 4800 RPM, WOT condition, is shown in Figures 4 and 5. Convective temperature predictions reflect the spark plug offset and the earlier and more prolonged contact between the flame and the piston zone 23.

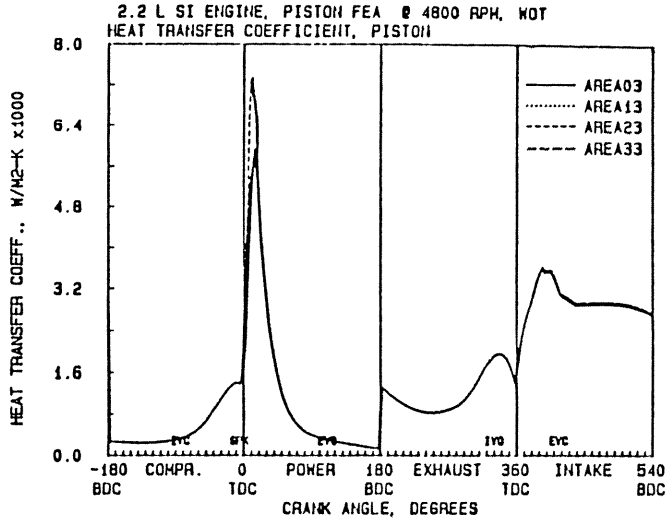

Figure 4. Convective heat transfer coefficients on piston inner surfaces 3, 13, 23 and 33; 4800 RPM, WOT.

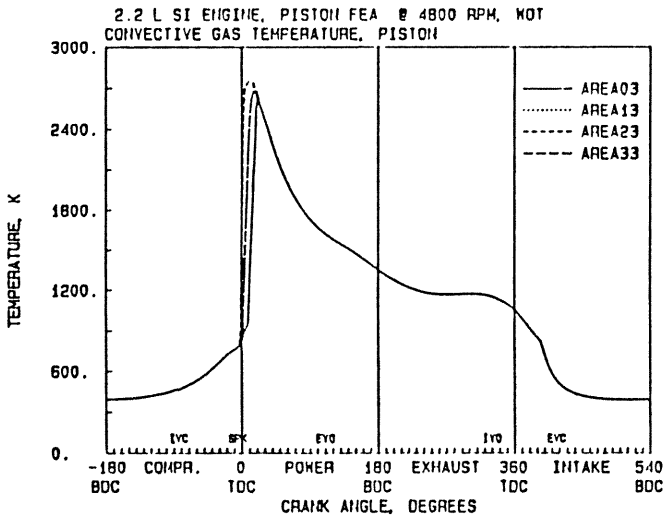

Figure 5. Convective gas temperature on piston outer surfaces 3, 13, 23 and 33; 4800 RPM, WOT.

The heat generated by ring-cylinder friction and piston skirt-cylinder friction is also computed. This heat is deposited on the affected piston, cylinder and ring surfaces which are in sliding contact in a manner consistent to where and when it has been generated.

The piston skirt and rings also provide a heat path from the piston to the cylinder. The thermal resistance (or conductance) through each ring was computed based on ring width and thermal conductivity, nominal ring contact areas with the ring groove and the cylinder, and a nominal oil film thickness and oil thermal conductivity. This conductance was then distributed in the form of scalar thermal elements between ring nodes and cylinder nodes. The distribution is consistent with the fraction of time areas associated with each ring node having contact with those associated with cylinder nodes. The skirtcylinder thermal interaction is established in a similar manner. The nominal heat transfer coefficient utilized for skirt-to-cylinder interaction was 6000 W/m^{2}K and was based on the skirt-cylinder clearance and oil thermal conductivity.

Finally, the crankcase side (oil/air cooling) boundary conditions were supplied as input, in the form of convective temperatures and heat transfer

coefficients. The convective temperature for surfaces exposed to oil splashing was set to 345-352 K based on the experimental input. For the splashing heat transfer coefficient, levels of 1000-3000 W/m^2 were used, depending on the location. These are levels generally associated with splashing of oil on piston undersurfaces. The lower level above was used for areas shielded from direct splashing such as the cavity between the pin boss and the piston crown. The higher level was applied to the undercrown surface. For the coolant passages around the cylinder and in the head, heat transfer coefficients of 4000 W/m^2K were applied, with a coolant temperature of 353 K.

PISTON TEMPERATURE DISTRIBUTION

Predicted piston temperatures are output by IRIS in a format identical to the ANSYS code, and these were post-processed to generate temperature contour plots on surfaces and sections of the piston. Temperature predictions for the 4800 RPM WOT condition are shown in Figures 6 and 7 in the form of temperature contours on orthographic views of the piston FE model. Peak piston temperature is 572 K and 520 K, respectively, for the 4800 RPM and 3000 RPM, WOT conditions.

For both conditions the highest temperature is near the center of the piston top surface. The cutback pin bosses on the front and back ends of the piston undercrown appear to act as conduction heat paths and to reduce temperature in the front and back sides of the piston. As a result, the temperature contours are elongated in the thrust plane. Closer analysis also indicated some differences between major thrust and minor thrust sides. The valve cutout is seen to cause higher temperatures on the piston surface at the sharp outer corner of the cutout. Within the cutout itself temperature drops toward the inner sharp corner as piston crown thickness decreases. Spark plug offset also slightly affects the profiles. As a result of higher convective temperatures (see Table I) on the minor thrust side toward which the spark plug is offset, temperatures on this side are seen to be a few degrees higher on the average. All of the above are relatively minor details of the temperature profile on the piston top, which is rather uniform with a variation of only 15-35 K.

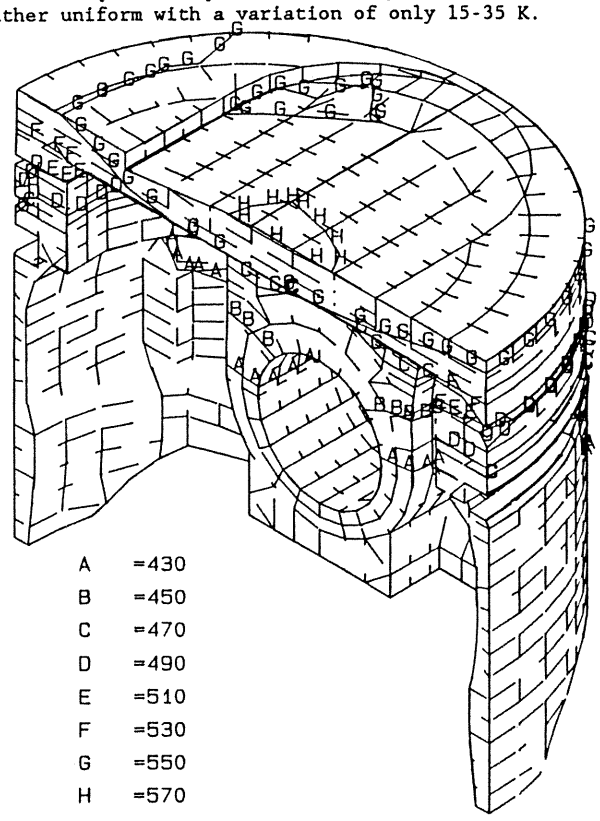

Figure 6. Orthographic inside view of piston temperature contours; 4800 RPM, WOT (in deg K).

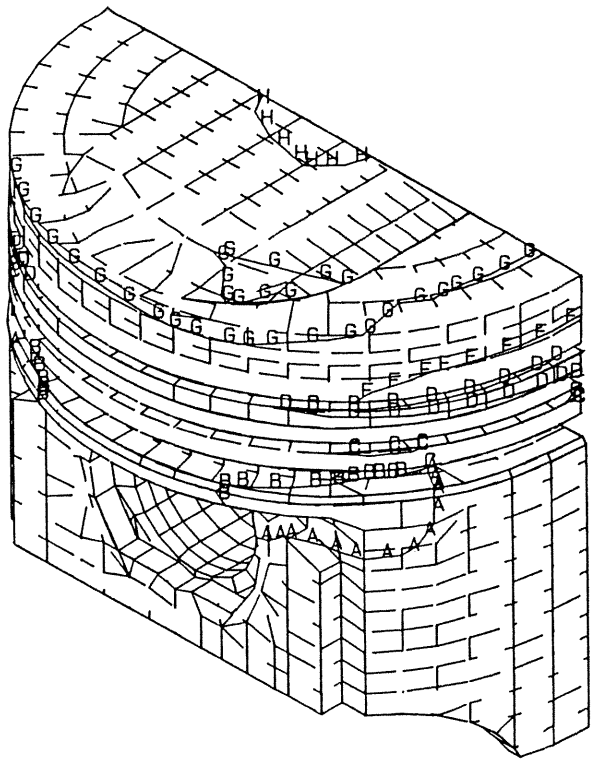

Figure 7. Orthographic outside view of piston temperature contours; 4800 RPM, WOT (in deg K).

In the central section of the piston in the thrust plane, the temperature is seen to drop rapidly in the ring zones, reflecting cooling both by oil splashing on the piston underside and by conduction to the cylinder through rings. The temperature distribution on lands and skirt of the piston is seen in Figure 7 as viewed from the front (or back). The effect of reduced cooling of the piston on the front and back due to the absence of a skirt there is evident. The temperature is more or less uniform circumferentially for the first and second lands. On the other hand, there is a significant circumferential temperature variation under the oil ring groove.

COMPARISON OF PREDICTIONS TO DATA

The predicted temperature distributions were compared to the data obtained by Furuhama (1989) at the same two engine speeds. The comparisons are shown in Figure 8, which displays three sketches of the piston. The top sketch is the view of the piston top, the central sketch is a cut through the plane of symmetry from the minor thrust side to the major thrust side. The bottom sketch is a side view, looking at the skirt and land surfaces from the "back side". The experimental data are shown in °C, and it is followed by the predicted result (also in °C) separated by a slash. The top sketch compares temperatures measured on the front and back surfaces; the predicted results are identical by reason of assumed symmetry. The central sketch compares measurements at six different locations on the piston crown, in the ring zone and in the skirt. Three additional locations are represented in the bottom sketch.

As can be seen, the level of agreement between the two sets of temperatures in general is very good. The exception is the center of the bottom sketch where the piston land area temperature is 20K higher in the experiment than in the prediction. This is also the area where cylinder cooling is reduced due to siamese bore construction. As mentioned above, this feature was not represented in the coarse cylinder model utilized in this study.

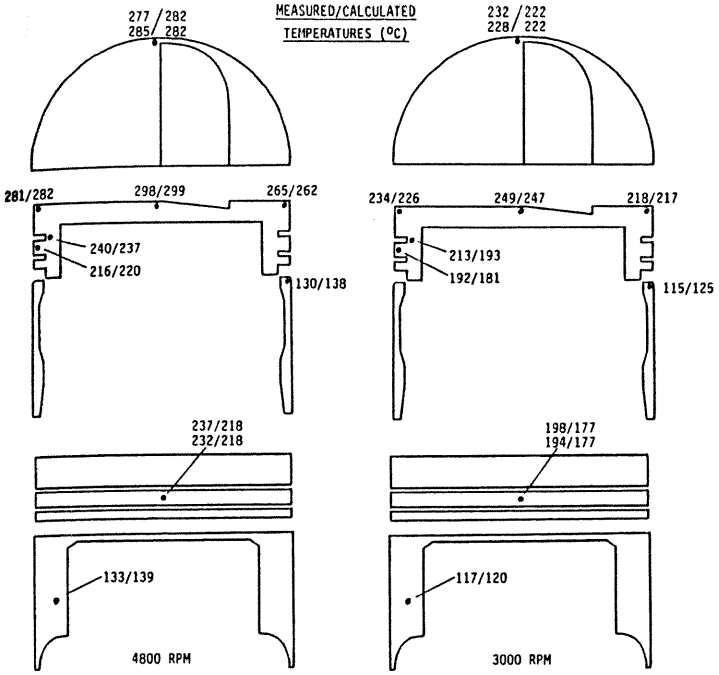

Figure 8. Comparison of piston temperature predictions and measurements at 4800 and 3000 RPM, WOT conditions.

THERMAL BALANCE AND HEAT PATHS

An important issue in engine design is the manner in which the heat, deposited on the piston by combustion chamber gases and by friction, is carried away from the piston. It influences the design of cylinder cooling passages and of oil cooling, which typically require design iterations to achieve a satisfactory result. This issue is best discussed in terms of the heat balance on the piston, which is formed as a result of numerous interactions and heat paths, and it requires careful analysis to interpret.

A quantity often referred to in the context of thermal design of pistons and selection of piston cooling strategy is the heat transferred from the piston to the cylinder coolant as a fraction of the total thermal load on the piston. Although this concept appears to be simple, a closer analysis shows it to be difficult.

The first attempt to express the fraction of piston thermal load which goes to the coolant might be the ratio of heat carried away by the cylinder coolant (q_{cool}) to the thermal load applied by the combustion gases on the piston top (q_{gasp}). Similarly, one may define a fraction of heat which is carried away by the oil from the piston underside (q_{oilp}) to the same thermal load q_{gasp}. These ratios will be termed "heuristic", i.e., based only on intuition and not based on rigorous analysis. Table III shows the results for the two operating points studied here, where all fluxes are defined positive for directions into the components. The first of the two ratios is seen to be larger than unity, and the sum of the two is 2.23 and 1.97, respectively, for the two engine conditions. This indicates quite clearly that the simple heuristic definition is imprecise and not very useful.

Table III. Heuristic Piston Cooling Ratios
(all heat fluxes are in W)

	q_{gasp}	q_{cool}	q_{oilp}	Heuristic Ratio Coolant[1]	Oil[2]
4800 rpm	4020	-6557	-2430	1.63	0.60
3000 rpm	2590	-3888	-1212	1.50	0.47

[1] $-q_{cool}/q_{gasp}$ [2] $-q_{oilp}/q_{gasp}$

It is thus necessary to analyze the piston/cylinder assembly as a complete system, as done in Figure 9, which introduces four other heat loads and heat paths: gas thermal load on the cylinder (q_{gasc}), oil thermal load on the cylinder (q_{oilc}), frictional heat (q_{fric}) and thermal load from the head contact (q_{head}); all of these were neglected in the heuristic definitions. Table IV lists the values for all of these additional quantities plus a cylinder-to-piston heat path (q_{cp}), to be defined later in Figure 10.

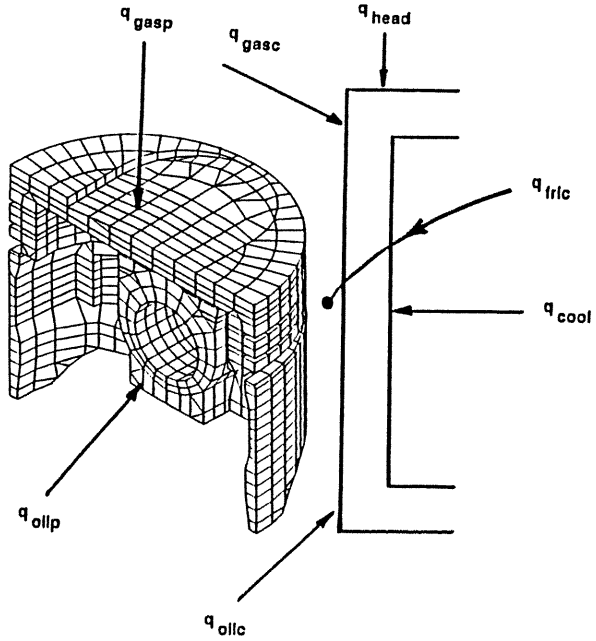

Figure 9. Schematic of heat paths in the piston/cylinder system.

Table IV. Additional heat loads and heat paths
(all heat fluxes are in W)

	q_{gasc}	q_{oilc}	q_{fric}	q_{head}	q_{cp}
4800 rpm	2570	-237	3210	-606	-3210
3000 rpm	1550	-134	1540	-446	-2148

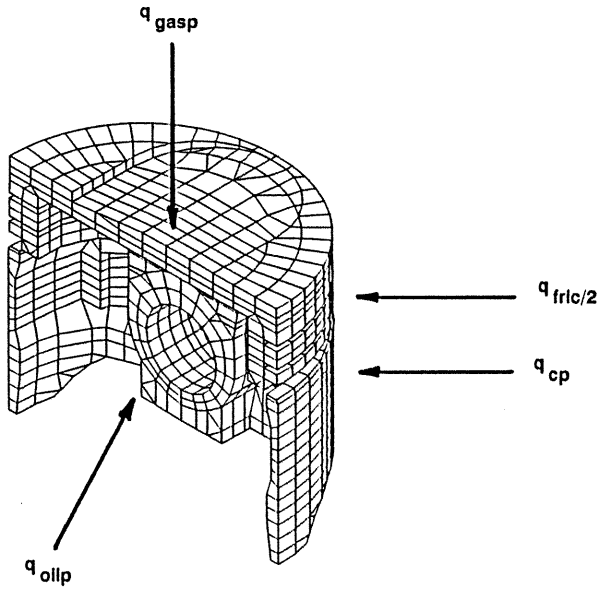

Figure 10. Schematic of a piston free body system.

The sought ratio describing the piston cooling modes has to take appropriately into account all seven of these loads and heat paths. That is not a precise task, as there are a number of different ways to proceed. Having experimented with a number of approaches, the authors settled on two definitions. One definition refers to the whole piston/cylinder system as defined in Figure 9, and considers the split of the gas heat load acting on the piston and the cylinder plus friction heat. From the overall balance this load splits into heat going in three directions: to the coolant, to the oil and to the head (any one of these could in principle be positive or negative). The sum of the three ratios is by definition unity, as can be seen in Table V. The split for this engine is seen to be over two-thirds to the coolant, about one quarter to the oil and 6-8% to the head.

Table V. Recommended Heat Transfer Ratios

	Piston/Cylinder System			Piston Free Body	
	Coolant[1]	Oil[2]	Head[3]	Cylinder[4]	Oil[5]
4800 rpm	0.67	0.27	0.06	0.57	0.43
3000 rpm	0.68	0.24	0.08	0.64	0.36

$q_1 = q_{gasp}+q_{gasc}+q_{fric}$ $\quad q_2 = q_{gasp}+\frac{1}{2} q_{fric}$

$^1 - q_{cool}/q_1$ $\quad ^4 - q_{cp}/q_2$

$^2 - (q_{oilp}+q_{oilc})/q_1$ $\quad ^5 - q_{oilp}/q_2$

$^3 - q_{head}/q_1$

Another definition refers to the piston force body diagram in Figure 10, which considers the split of the gas heat load applied to the piston top plus half of the friction heat (the other half may be assumed to be deposited on the cylinder). From the overall balance this heat load splits in two directions: to the cylinder surface (q_{cp}) and to the piston undersurface. Again, the sum of the two ratios is by definition unity, see Table V. The split for this engine is about 60/40 between the two paths.

The inclusion of the friction heat in the above analysis is essential. The friction heat is a large part of the overall heat load, as it represents 33% of the total thermal load at 4800 rpm and 27% at 3000 rpm (see Tables III and IV), and it must be considered in any analysis of piston cooling loads. To assess its contribution and determine the heat paths for its dissipation from the system, a parallel analysis was made of a "frictionless" engine in which the frictional heat load was set to zero. From the differences in the various heat loads and heat paths it was determined that the frictional heat load was being carried away in about the same proportions for both of the operating conditions: 72% to coolant and 15% piston oil cooling and smaller fractions to gas side, to head and to cylinder oil cooling. The analysis also showed that the frictionless engine had lower peak piston temperatures, by 14 K at 4800 rpm and by 9 K at 3000 rpm. The fact that much of the friction heat load is immediately carried away by the coolant explains why the change of piston temperatures due to its presence is not too large. This would not be so if the engine were operated in an uncooled mode (with no cylinder cooling).

The main purpose of this discussion was to define meaningful parameters to be used in the evaluation of piston cooling alternatives, and to identify the importance of frictional heat deposition. It should be stressed that the above results are specific to a given engine, details of the cylinder block and piston cooling, materials used and level of friction between the piston and cylinder. Thus the ratios calculated for this engine should not be viewed as typical or universal.

CONCLUSIONS

1. An analysis was carried out of heat flow patterns in a piston using a simulation which directly couples the prediction of engine performance with the solution of FE structure heat conduction.
2. The predictions of temperature distributions were compared to detailed experimental temperature data, and the agreement was found to be good.
3. Analysis of the heat paths in the piston/cylinder assembly was carried out. A total of seven heat loads and paths were identified and a set of ratios quantifying the split of the cooling loads was proposed. It showed that for the assembly about two-thirds of the applied heat load was directed to the cylinder coolant and about one quarter to the piston underside oil cooling.
4. A second analysis assessed the heat loads acting on the piston alone with four heat loads and paths involved. Again ratios expressing the flow of heat to the cylinder and to the piston underside were proposed. These showed an approximate 60/40 split between cylinder and piston underside.
5. Finally, an analysis was made of the role frictional heat deposition plays. The friction was responsible for 33% and 27%, respectively, of the total heat load at the two operating conditions. Its presence has to be accounted for to calculate correctly the cooling loads and also the resultant piston temperatures. Most of the frictional heat load was seen to be directed to the cylinder coolant (72%) and less to the piston undercrown cooling (15%).

REFERENCES

Furuhama, S. (1989), "Piston Temperature Measurement", Musashi Institute of Technology, Engine Research Laboratory, Report to Chrysler Corporation.

Groeneweg, M. A., Ahuja, R., Pfeiffer, R. F. and Bezue, T. N. (1987), "Current Applications of Finite Element Analysis to Diesel Engine Component Design", SAE Paper 870813.

Hosokawa, T., Tsukada, H., Maeda, Y., Nakakubo, T. and Masahiko, N. (1989), "Development of Computer-Aided Engineering for Piston Design", SAE Paper 890775.

Keribar, R., Morel, T. and Toaz, M. (1990), "An Investigation of Structural Effects of Fiber Matrix Reinforcement in Aluminum Diesel Pistons", SAE Congress, Detroit, SAE Paper 900536.

Keribar, R. and Morel, T. (1987), "Thermal Shock Calculations in I.C. Engines", SAE Congress, Detroit, SAE Paper 870162.

Li, C. H. (1988), "Thermal and Mechanical Behavior of an L-4 Engine", SAE Paper 881149.

Li, C. H. (1982), "Piston Thermal Deformation and Friction Considerations", SAE Paper 820086.

Morel, T. and Keribar, R. (1985), "A Model for Predicting Spatially and Time Resolved Convective Heat Transfer in Bowl-in-Piston Combustion Chambers", SAE Congress, Detroit, SAE Paper 850204.

Morel, T. and Wahiduzzaman, S. (1987), "Effect of Speed, Load, and Location on Heat Transfer in a Diesel Engine - Measurements and Predictions", SAE Congress, Detroit, SAE Paper 870154.

Morel, T., Keribar, R. and Blumberg, P. N. (1988A), "A New Approach to Integrating Engine Performance and Component Design Analysis Through Simulation", SAE Congress, Detroit, SAE Paper 880131.

Morel, T., Rackmil, C. I., Keribar, R. and Jennings, M. J. (1988B), "Model for Heat Transfer and Combustion in Spark Ignited Engines and Its Comparison with Experiments", SAE Congress, Detroit, SAE Paper 880198.